Nutrition and Cancer

ISSN: 0163-5581 (Print) 1532-7914 (Online) Journal homepage: http://www.tandfonline.com/loi/hnuc20

Allium Roseum L. Extract Exerts Potent Suppressive Activities on Chronic Myeloid Leukemia K562 Cell Viability Through the Inhibition of BCR-ABL, PI3K/Akt, and $ERK_{1/2}$ Pathways and the Abrogation of VEGF Secretion

Soumaya Souid, Hanen Najjaa, Ichrak Riahi-Chebbi, Meriam Haoues, Mohamed Neffati, Ingrid Arnault, Jacques Auger, Habib Karoui, Makram Essafi & Khadija Essafi-Benkhadir

To cite this article: Soumaya Souid, Hanen Najjaa, Ichrak Riahi-Chebbi, Meriam Haoues, Mohamed Neffati, Ingrid Arnault, Jacques Auger, Habib Karoui, Makram Essafi & Khadija Essafi-Benkhadir (2016): Allium Roseum L. Extract Exerts Potent Suppressive Activities on Chronic Myeloid Leukemia K562 Cell Viability Through the Inhibition of BCR-ABL, PI3K/Akt, and $ERK_{1/2}$ Pathways and the Abrogation of VEGF Secretion, Nutrition and Cancer, DOI: 10.1080/01635581.2017.1248295

To link to this article: http://dx.doi.org/10.1080/01635581.2017.1248295

Published online: 28 Nov 2016.

NUTRITION AND CANCER
2016, VOL. 0, NO. 0, 1–14
http://dx.doi.org/10.1080/01635581.2017.1248295

Taylor & Francis
Taylor & Francis Group

Allium Roseum L. Extract Exerts Potent Suppressive Activities on Chronic Myeloid Leukemia K562 Cell Viability Through the Inhibition of BCR-ABL, PI3K/Akt, and $ERK_{1/2}$ Pathways and the Abrogation of VEGF Secretion

Soumaya Souid[a,b], Hanen Najjaa[c], Ichrak Riahi-Chebbi[a,b], Meriam Haoues[b,d], Mohamed Neffati[c], Ingrid Arnault[e], Jacques Auger[f], Habib Karoui[a,b], Makram Essafi[b,d], and Khadija Essafi-Benkhadir[a,b]

[a]Institut Pasteur de Tunis, LR11IPT04 Laboratoire d'Epidémiologie Moléculaire et de Pathologie Expérimentale Appliquée Aux Maladies Infectieuses, Tunis, Tunisie; [b]Université de Tunis El Manar, Tunis, Tunisie; [c]Laboratoire d'Ecologie Pastorale, Institut des régions Arides de Médenine, Tunisie; [d]Institut Pasteur de Tunis, LTCII LR11IPT02, Tunis, Tunisie; [e]CETU Innophyt, Université François Rabelais, avenue Monge, France, Tours; [f]IRBI, UMR CNRS 6035, Université François Rabelais, avenue Monge, France, Tours

ABSTRACT

Use of plant extracts, alone or combined to the current chemotherapy as chemosensitizers, has emerged as a promising strategy to overcome tumor drug resistance. Here, we investigated the anticancer activity of *Allium roseum* L. extracts, a wild edible species in North Africa, on human Chronic Myeloid Leukemia (CML) K562 cells. The dehydrated aqueous extract (DAE) disturbed the cell cycle progression and induced the apoptosis of K562 cells. Chemical analysis of DAE showed a diversity of organosulfur compounds S-alk(en)yl-cysteine sulfoxides (RCSO) and high amount of allicin, suggesting that such molecule may be behind its antitumor effect. DAE was efficient in inhibiting K562 cell viability. DAE inhibitory effect was associated with the dephosphorylation of the BCR-ABL kinase and interfered with $ERK_{1/2}$, Akt, and STAT5 pathways. Furthermore, we found that DAE-induced inactivation of Akt kinase led to the activation of its target FOXO3 transcription factor, enhancing the expression of FOXO3-regulated proapoptotic effectors, Bim and Bax, and cell cycle inhibitor p27. Finally, we found that DAE reduced the secretion of vascular endothelial growth factor. Overall, our data suggest that *A. roseum* extract has great potential as a nontoxic cheap and effective alternative to conventional chemotherapy.

ARTICLE HISTORY
Received 20 January 2016
Accepted 4 August 2016

Introduction

Chronic myelogenous leukemia (CML) is a malignant disorder of the hematopoietic stem cells characterized by the presence of a balanced genetic translocation of chromosomes 22 and 9 (1). The translocation results in formation of the BCR-ABL fusion oncogene encoding a protein with constitutive tyrosine kinase activation, which plays a central role in the pathogenesis of the disease. The chimeric protein BCR-ABL activates a variety of downstream effectors and signaling pathways, including the Ras/Raf/MEK/ERK, STAT, and PI3K/Akt pathways, leading to growth factor-independent cell cycle progression, failure to differentiate, inhibition of apoptosis, alterations in cell-cell and cell-matrix interactions, and leukemogenesis (2). Once activated, the PI3K controls cell growth, proliferation, and apoptosis, as well as steps that are involved in tumor formation and malignant cell dissemination through secretion of proangiogenic vascular endothelial growth factor (VEGF) (3). The extracellular signal-regulated kinase (ERK) is one of the most important signaling pathways involved in the regulation of cell proliferation and differentiation, and protects cells against apoptosis (4). Imatinib Mesylate (IM previously known as Gleevec or STI571) is a BCR-ABL tyrosine kinase inhibitor (TKI) that competes with the ATP-binding site of BCR-ABL and stabilizes the oncoprotein in its inactive conformation, thereby inhibiting its TK activity. This drug potently induces growth arrest, apoptosis, and autophagy of BCR-ABL cells (5). However, the development of resistance to Imatinib has emerged as an important problem in patients with CML, most often due to acquired mutations in the target kinase (6) indicating that there is an urgent need for the development of novel therapeutic strategies.

Exploring natural products have become an approach for identification of novel clues for leukemia therapy.

CONTACT Khadija Essafi-Benkhadir essafi.khadija@pasteur.rns.tn; khadija.benkhadir@yahoo.fr Laboratoire d'Epidémiologie Moléculaire et de Pathologie Expérimentale Appliquée Aux Maladies Infectieuses (LR11IPT04), Institut Pasteur de Tunis, 13 Place Pasteur BP 74, 1002 Tunis– Belvédère, Tunisia.

Color versions of one or more of the figures in the article can be found online at www.tandfonline.com/hnuc.

Medicinal benefits of the vegetables of genus *Allium* (e.g., garlic) have been documented throughout the recorded history (7). Evidence from epidemiological studies showed that there is a significant correlation between *Allium* spp. intake and healing of several diseases such as decreasing the risk of carcinogenesis (8). *Allium roseum* is a highly variable species represented in North Africa by 12 different taxa: 4 varieties, 4 subvarieties, and 4 forms. In Tunisia, Cuénod (9) and Le Floc'h (10) described only three varieties: var. *grandiflorum*, var. *perrotii*, and var. *odoratissimum*. Odoratissimum was considered as an endemic taxon in North Africa. This author reported that this variety is a perennial spontaneous weed and was used since ancient times by local consumers as a vegetable, spice, and herbal remedy. Its edible aerial parts are widely harvested and sold commercially (11).

In fact, the fresh young leaves and bulbs of *A. roseum* are consumed in salad and used as spice to prepare traditional recipes. Besides its culinary use, *A. roseum* is also used in folk medicine for the treatment of headaches, stomach aches, and rheumatism (10). Phytochemical screening of *A. roseum* organic and aqueous extracts revealed the presence of bioactive compounds such as saponins, tannins, flavonoids, coumarins, steroids, cardiac glycosides, free quinone, and iridoids (12,13). Recently, we showed that *A. roseum* possesses strong antioxidant and antimicrobial activities (14,13). However, its anticancer activity has not yet been characterized. Thus, in the present study we investigated for the first time the antiproliferative effect and the mechanism of action of *A. roseum* on human CML cell line (K562).

Materials and methods

Plant material and extracts preparation

The whole plants of wild-growing *A. roseum* were collected from the arid South-East of Tunisia (Bengardane), at the vegetative stage of the plant growing cycle (January, 2010). Botanical identification was made by Dr. Mohamed Neffati Director of the Range Ecology Laboratory of the "Institut des Régions Arides," Tunisia (I.R.A.), according to the "Flora of Tunisia" (9). Voucher specimens were deposited at the herbarium of the I.R.A. 5 g of dried and ground leaves of *A. roseum* were extracted separately with 50 mL of methanol (DME) and distilled water (DAE). 5 g of fresh *A. roseum* were extracted separately with 10 ml of methanol (FME) and distilled water (FAE) during 1 h at room temperature. After centrifugation at 8,000 *g*, supernatants were recovered. To prevent denaturation, extraction was achieved rapidly and extracts were immediately used or stored at −20°C until further use.

Quantitative HPLC-UV analysis of the selected organosulfur compounds

The very large biocide effect of *Allium* is closely related to complex biochemistry of sulfur compounds (15). In addition to common sulfur amino acids such as cysteine, cystine, methionine, glutathione, and peptide derivatives, *Allium* spp. contain S-alk(en)yl-cysteine sulfoxides (RCSO), named the aroma precursors that give thiosulfinates and corresponding disulfides. The proportions of RCSO vary from the species, the organs, the varieties (16), and the environmental conditions (17). In the case of garlic, the major RCSO is alliin (S-allyl-L-cysteine sulfoxide) producing the allicin (diallyl thiosulfinate) responsible for the characteristic odor of garlic and rearranging fast in diallyl disulfide (DADS).

For that reason, we analyzed the RCSO presents in *A. roseum* preserved under both processes: crushed, dried, and stored at three temperatures (4°C, room temperature, and 35°C) for 3 mo (90 days). Analysis was performed after 7, 15, 30, 45, and 90 days of storage. Ion-pair HPLC and UV detection was used to quantify S compounds from dried and crushed *A. roseum* extract. This technique allows the quantification of the three organosulfur precursor (RCSO), (+)-*S*-(2-propenyl)-L-cysteine sulfoxide (alliin) (AICSO), (+)-*S*-(trans-1-propenyl)-L-cysteine sulfoxide (isoalliin) (PeCSO), and (+)-S-methyl-L-cysteine sulfoxide (methiin) (MCSO) (18).

Then, samples were extracted under allinase inhibiting condition separately. First, 1 g of dried and 5 g of crushed *Allium* were extracted at room temperature with 90 ml and 10 ml respectively, of methanol-water (80:20, v/v) and 0.05% formic acid (pH < 3). An aliquot was diluted five times and filtrated (0.2 μm), and 10 μL was analyzed by HPLC. HPLC analysis was carried out using a Waters 616 pump and a DAD 996 diode-array detector (Waters,

Milford, MA, USA). Compounds were separated on a 150× 3 mm I.D, 3 μm particle Hypurity Elite C18 column Thermo Quest, at 38°C (Thermo Hypersil, Keystone, Bellefonte, PA, USA) and UV detector operated at 208 nm. The column flow rate was 0.4 ml/min. The mobile phase consisted of: (A) 20 mM sodium dihydrogen phosphate + 10 mM heptanesulfonic acid, pH 2.1 (adjusted with orthophosphoric acid 85%); and (B) acetonitrile −20 mM sodium dihydrogen phosphate + 10 mM heptane sulfonic acid, pH 2.1 (50:50, v/v). The gradient program was previously

described (18). Data acquisition is performed using Millennium software from Waters. Sulfur compounds were identified by the comparison of their retention times and their spectra with standard compounds (18).

Allicin determination

Allicin, diallylthiosulfinate, is an organosulfur compound known for its effective medicinal properties (19-21). Many reports attribute the cell death in various cancer cell lines and inhibition of induced tumor in vivo to the anticancer action of allicin (22,23). For that reason, we determined the allicin content in aqueous *A. roseum* extracts. Two grams of each sample was blended in 40 ml of distilled water, and crushed with mortar and pestle. The mixture was centrifuged at 5,000 rpm and filtrated under 0.45 μm. The allicin content was extracted and determined according to Miron et al. (24). Briefly, 20 μl of the filtered aqueous extract and 30 μl of water were incubated at room temperature in 1 ml of 4-mercaptopyridine (10^{-4} M), 100 mM Na-phosphate buffer and 10 mM EDTA, pH 7.2 for 30 min, resulting in the formation of a mixed disulfide, 4-allylmercaptothiopyridine, and a consequent shift in absorbance at 324 nm was monitored. The ε_M value used for allicin concentration calculation was 39,600 M^{-1} cm^{-1} at 324 nm. The allicin concentration was calculated against a distilled water blank, using the following formula:

$$[\text{Allicin}] = [\,\text{OD}_{324}\,(\text{Blank}) - \text{OD}\,(\text{Extract})]$$

$$\times\ \text{Dilution factor}\ /\ \varepsilon_M.$$

Cell culture and reagents

The human leukemia K562 cell line was obtained from the American Tissue Culture Collection (Rockville, MD, USA). Cells were cultured under standard conditions and were grown at 37°C under 5% CO_2 in RPMI 1640 medium supplemented with FBS (10%, v/v), streptomycin (100 μg/ml), penicillin (100 U/ml), and 1 mM sodium pyruvate. Cell viability was assessed by trypan blue exclusion assay.

The phospho-Akt, Akt, Bax, Bim, cleaved caspase 8, $ERK_{1/2}$, phospho-FOXO3, PARP, procaspase 9, and Actin antibodies were from Cell Signaling Technology (Danvers, MA, USA). Anti-phospho-$ERK_{1/2}$ were from Sigma-Aldrich (L'Isle d'Abeau, Chesnes, France), and anti-ERK2 and anti-HSP90 were from Santa Cruz Biotechnology (Santa Cruz, CA). Anti-horseradish peroxidase-conjugated anti-mouse and anti-rabbit antibodies were from Promega (Madison, WI).

Measurement of cell viability

Cell viability was measured by 3-(4, 5-dimethylthiazol-2-yl)-2,5-diphenyltetrazolium bromide (MTT) and trypan blue exclusion assays.

MTT assay

Cells were seeded in 96-well plates at a density of 6×10^3 cells per well and treated with different concentrations of *A. roseum* extracts (ranging from 10 to 900 μg/ml). After incubation during 24 h and 72 h, fifty microliters of MTT reagent (1 mg/ml) was added to cells followed by incubation during 3 h at 37°C. Then, the formazan crystals formed were solubilized by adding 100 μl DMSO. Absorbance of the formazan dye produced by metabolically active cells was measured at 540 nm with a microplate reader (MULTISKAN, Labsystems). The data were presented as percentage of viable cells (%). Each data point presented the average of three independent experiments.

Trypan blue exclusion assay

The mock and treated cells were stained with 0.4% (w/v) trypan blue and counted under an inverted light microscope. Each condition had three repeats of counting. The cell viability (%) was calculated using the following formula: (number of viable cells (unstained) in treated group/number of total viable cells in the control group)$\times$ 100. Each data point presented the average of three independent experiments.

Determination of cell cytotoxicity: LDH release

The loss of membrane integrity was evaluated via the lactate dehydrogenase (LDH) assay. LDH release from cells was determined by the LDH Cytotoxicity Detection Kit-PLUS test (Roche Applied Science, Mannheim, Germany) according to the manufacturer's protocol detection kit (Roche Boehringer Mannheim, Rueil-Malmaison France) as an index of toxicity. Cells were seeded (10^5 cells/well in 12-well plates) and cultured for 72 h with different concentrations of DAE (300, 600, and 900 μg/ml). The supernatant of treated cells, and negative (mock) and positive controls (Triton 1%) were used for the enzymatic assay. The assay procedure was performed according to the instruction included in the kit. The results were expressed as a percentage of 1% Triton X-100 that induced LDH release (100% toxicity). Cytotoxicity (%) = (DAE experimental value–negative control value)/(positive control value–negative control value)$\times$ 100.

Cell death analysis

Observation of morphologic changes

K562 cells were seeded into six well plates and treated with (300, 600, and 900 μg/ml) DAE for 24 h. The cellular morphological changes induced by different concentrations of DAE were observed using a phase contrast microscopy.

Apoptosis detection

Detection and quantification of apoptosis was performed by the analysis of phosphatidylserine on the outer leaflet of apoptotic cell membranes using Annexin V/PE apoptosis detection kit (BD-Pharmingen) according to the manufacturer's protocol. Approximately 10^5 cells, treated with different concentrations of DAE and 10 μM Staurosporine as a positive control were collected by centrifugation, and washed with PBS (1X). K562 cells were suspended in 100 μl of binding buffer (1X) before addition of 4 μl of Annexin V conjugated to phycoerythrin (PE) and 4 μl of 7-AAD. The cell suspension was incubated in the dark rapidly for 15 min. Stained cells were analyzed on a Becton Dickinson FACScanto II flow cytometer and further analyzed with BD FACS Diva 6 software (Becton Dickinson). Cell death was quantitatively evaluated by measuring the proportion of Annexin V-positive cells, regardless of their staining for 7-AAD in order to include both apoptotic and necrotic cell death. Values are given in percent of total cell number. Percentage of apoptotic cells (%) was calculated as follows: early apoptotic cells (%) +late apoptotic (%).

Cell cycle analysis

After 24 h of treatment with IM at 1 μM and DAE at 300 μg/ml, the cells were washed twice with cold phosphate-buffered saline (PBS-2% bovine albumin serum) and then centrifuged at 1,000 rpm. To permeabilize the cell membrane, 500 μl of Hypretonic-Triton Buffer (20 mM HEPES, pH = 7.2; 0.16 M NaCl; 1 mM EGTA; 0.05% Triton X-100) was added to cell pellets and then rapidly incubated on ice for 1 min. After centrifugation, cell pellets were resuspended in propidium iodide (PI)/RNase staining solution (Cell Signaling Technology; Danvers, MA) and incubated for 30 min in the dark. Cell cycle progression was analyzed by on a Becton Dickinson FACScanto II flow cytometer and further analyzed with BD FACS Diva 6 software (Becton Dickinson). The PI fluorescence signal at FL2-A peak versus counts was used to determine cell cycle distribution.

Western blotting analysis

Cell lysis, SDS-polyacrylamide gel electrophoresis (PAGE), and Western blotting protocols were performed according to standard procedures. After 24 h, cells were collected and lysed at room temperature with Laemmli buffer. Protein content was quantified using the BCA method (Bicinchoninic Acid Protein Assay kit, Sigma). Cell lysates were heated at 100°C for 5 min, centrifuged at 13,000 rpm for 15 min, and then supernatant was used for immunoblotting. Cell extracts were resolved by SDS-PAGE, and transferred onto a polyvinylidenedifluoride membrane (Immobilon-P; Millipore, Billerica, MA). The immunoreactive proteins were visualized by the enhanced chemiluminescence detection system (ECL; Millipore, Billerica, MA)

Determination of cytokine concentration

VEGF protein release was measured using an enzyme-linked immunosorbent assay (ELISA) kit (Quantikine; Thermo SCIENTIFIC) and normalized to cell number.

Statistical analysis

The experiments were performed in triplicates. All values were expressed as means ± S.E and Student's test was done to analyze significance of difference between different groups. Differences with p-values of less than 0.05 were considered statistically significant.

Results

Effect of the dried and fresh A. roseum extracts on the viability of human chronic myeloid leukemia cells

In order to assess whether *A. roseum* dried aqueous extract (DAE) and fresh aqueous extracts (FAE) affect the viability of leukemic cells, we treated the well-characterized human K562 cell line with increased concentrations of each extract (10, 50, 100, 200, and 500 μg/ml) for 72 h. The MTT assay showed that the DAE significantly reduced the proliferation of K562 cells in a dose-dependent manner. The highest antiproliferative effect of DAE was reached at the concentration of 500 μg/ml (87% of inhibition), while no effect, on cell proliferation, of the FAE was registered (Fig. 1A). To better explore the dried material, we have further used methanol as a polar solvent to prepare what we call dried methanolic extract (DME). However, this latter extract showed only a very moderate antiproliferative effect (lower than 20% of inhibition) on K562 cells, compared to the one found with DAE.

Phytochemical characterization of dried and fresh A. roseum

The organosulfur compounds (RCSO) were the most characterized constituents of *Allium* that mediate its

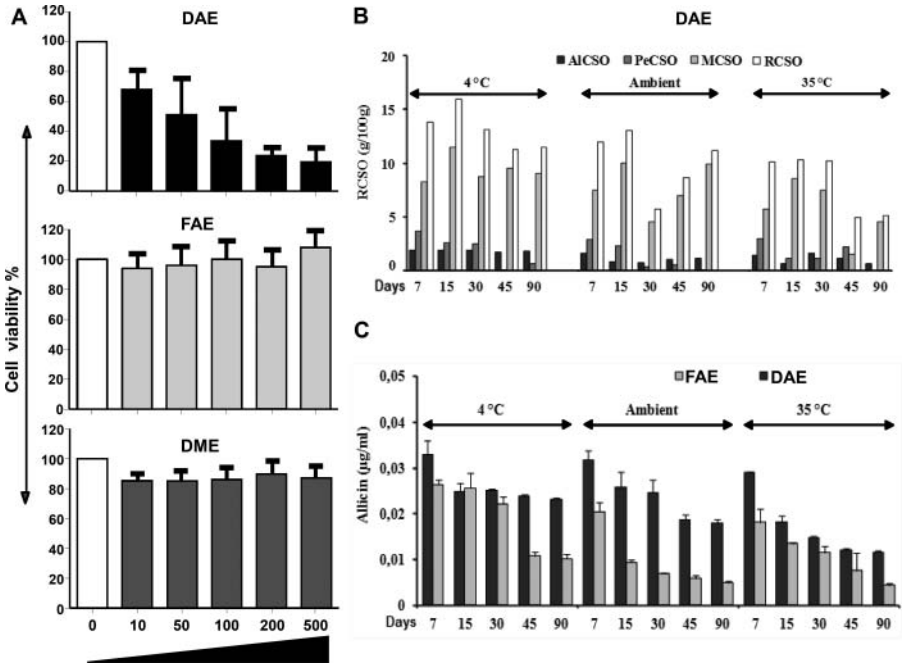

Figure 1. Assessment of the effect of fresh and dried *Allium roseum* extracts on K562 cells growth. A: Exponentially growing K562 cells were treated for 72 h with the indicated concentrations (0, 10, 50, 100, 200, and 500 μg/ml, respectively) of DAE, FAE, and DME. Cell survival/proliferation was assessed by MTT assay, B: The evolution of organosulfur compounds (RCSO) in dehydrated *A. roseum* stored at 4°C, room temperature, and 35°C during 90 days. AlCSO: (+)-*S*-(2-propenyl)-L-cysteine sulfoxide (alliin), PeCSO: (+)-*S*-(trans-1-propenyl)-L-cysteine sulfoxide (isoalliin), and MCSO: (+)-S-methyl-L-cysteine sulfoxide (methiin), C: The evolution of allicin content in dehydrated and crushed *A. roseum* stored at 4°C, room temperature, and 35°C during 90 days.

antitumor activity (25). In accordance with this, we suggested that the potent inhibitory effect of DAE on K562 cell viability could be associated to a typical profile of these compounds.

Based on the fact that preparation and storage conditions can adversely affect the quality of *Allium* extract (26), we analyzed the evolution of RCSO (aroma precursors) in DAE under different storage conditions (4°C, room temperature or at 35°C). Interestingly, in all tested conditions, the FAE extract does not contain Ti precursors, even a week after processing (Data not shown). In DAE, the total RCSO content decreased significantly in tested conditions and 4°C was considered as the best temperature for RCSO precursor's conservation (Fig. 1B). At this temperature, the level of organosulfur precursors reached 11.5 mmol/g (with only 4.4 mmol/g loss) even after 90 days of storage. In all tested conditions, AICSO (alliin) is more stable and its content is low compared to other RCSO precursors (Fig. 1B). MCSO (methiin) represented the highest amount of precursors and its level increased from 8.25 to 11 mg/mmol after 2 wk of storage. However, under different storage temperatures tested, PeCSO (isoaliin) was the most alterable compound. Its content decreased to 3.08, 2.77, and 2.99 mmol/g at 4°C, room temperature, and 35°C respectively (Fig. 1B).

Allicin, the product of the interaction of AICSO (alliin) with the enzyme alliinase, is the main biologically active component that mediates antitumor properties (27,28). As the changes in the allicin content were directly influenced by corresponding changes in alliin and alliinase (29), we asked whether the differential inhibitory effect between DAE and FAE on K562 cell proliferation could be attributed to the difference of allicin content. Interestingly, in all storage conditions, even if the concentration of allicin in two extracts decreased after 7 days, DAE presented the highest content of this compound compared to FAE even after 90 days (Fig. 1C). This result suggest that the antiproliferative effect of DAE could be associated to the high concentration of allicin in this extract, which could explain the decrease of AICSO (alliin) content in the same conditions (Fig. 1B, C).

DAE is effective against K562 cells and is devoid of toxicity

As DAE exhibited the highest growth inhibition on K562 cells after 72 h of treatment, we investigated its activity after a shorter period of treatment, 24 h. Three different concentrations ranging from 300 to 900 μg/ml of DAE were tested using two methods, the MTT assay and

trypan blue dye, to exclude any artifacts that may come from interaction of DAE with MTT, which could be directly reduced by this extract (30). Interestingly, we found that both methods showed similar results and that DAE significantly decreased K562 cell viability in a dose-dependent manner ($P < 0.05$) after a short kinetic during 24 h with an IC50 value around 300 μg/ml. However, treatment of the cells with 1 μM (0.6 μg/ml) of the currently used anti-CML drug, Imatinib, exerted only a 32% inhibition of cell growth (Fig. 2A, B). It is worth to note that the inhibitory effect of both DAE and Imatinib significantly ($P < 0.05$) increased and reached almost the same level 72 h post treatment (Fig. 2A, B). To better characterize the effect of DAE on K562 cells and check whether its use could induce cell toxicity, treated and mock cells were subjected to LDH assay after 72 h. The results showed no difference in LDH release between cells treated with DAE (300, 600, and 900 μg/ml) and mock-treated cells (0% of toxicity), while Imatinib (at 1 μM which corresponds to 0.6 μg/ml) and the positive control, Triton, induced, respectively, 18% and 100% toxicity. Hence, DAE is devoid of toxicity toward K562 cells after 72 h (Fig. 2C). Moreover, MTT and trypan blue exclusion assays showed that DAE, at 300 μg/ml, did not affect the viability of the nontumoral cells, the *NIH/3T3 Fibroblasts*, compared to 87 $\pm$ 3.8% and 97 $\pm$ 2.1% of inhibition observed, respectively, with 600 and 900 μg/ml (Fig. 2A, B). These data suggest that DAE is endowed with selective inhibitory effect. Moreover, DAE was even less toxic than Imatinib when the concentration of 300 μg/ml was used (Fig. 2B, C). This latter concentration of DAE was then selected for further experiments to explore the mechanisms by which DAE inhibited the cell growth of K562 leukemic cells.

DAE induces caspase-dependent apoptosis of K562 cells through both extrinsic and intrinsic pathways

Microscopic analysis of DAE-treated cells showed that the growth inhibitory effect was associated with the

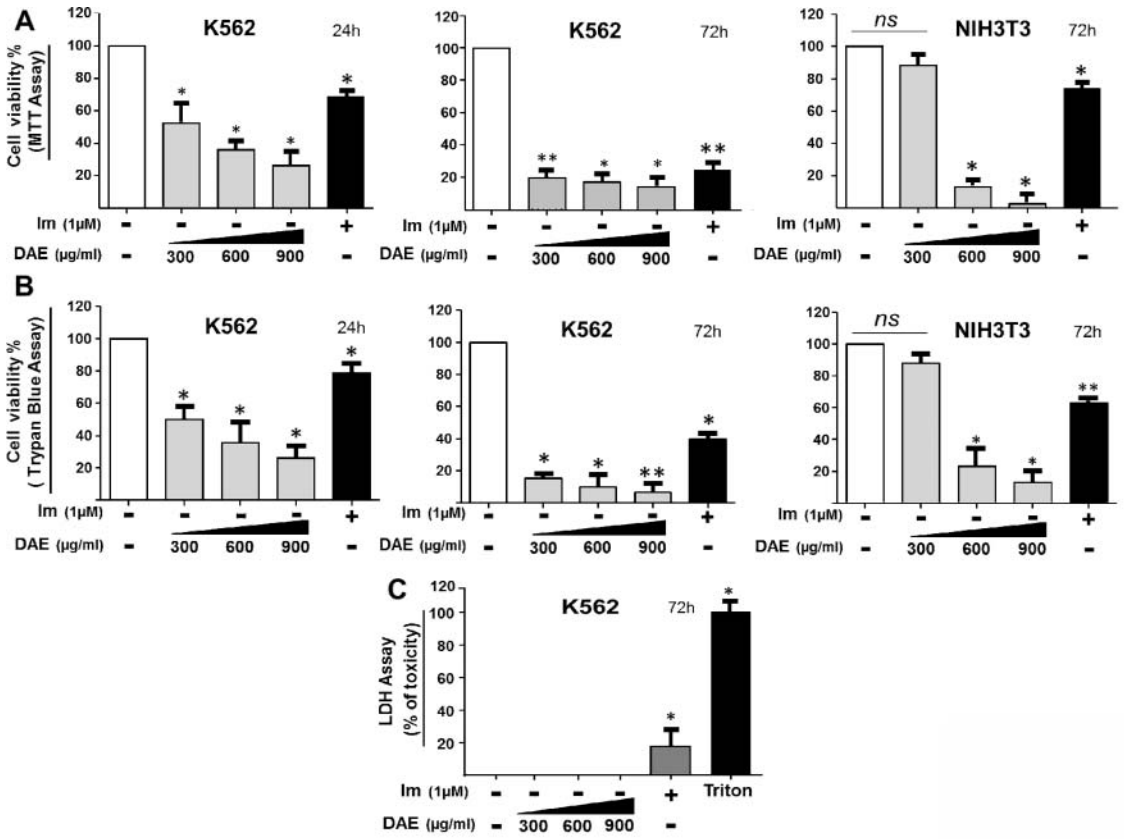

Figure 2. DAE exerted antileukemia effect without any toxicity on K562 cells and noncancerous cells NIH3T3. K562 and NIH3T3 cells were incubated with DAE (300, 600, and 900 μg/ml) or with 1 μM Imatinib (IM) for 24 and 72 h. At the end of incubation, MTT method A: and trypan blue exclusion assay B: were used to determine the cell survival rates. DAE exerted a dose- and time-dependent antiproliferative effect on K562 cells but it did not exert any effect on NIH3T3 viability at 300 μg/ml after 72-h treatment, C: LDH assay revealed that DAE at the same range of concentrations was devoid of toxicity toward K562 cells compared to the drug IM after 72 h of treatment. Results were normalized to each control in percentage and represented as mean $\pm$ SE of three independent experiments, each performed at least in triplicate. Statistical differences were analyzed with Student's *t*-test ($^{*}P < 0.05$, $^{**}P < 0.01$ as compared to the control, ns: not significant).

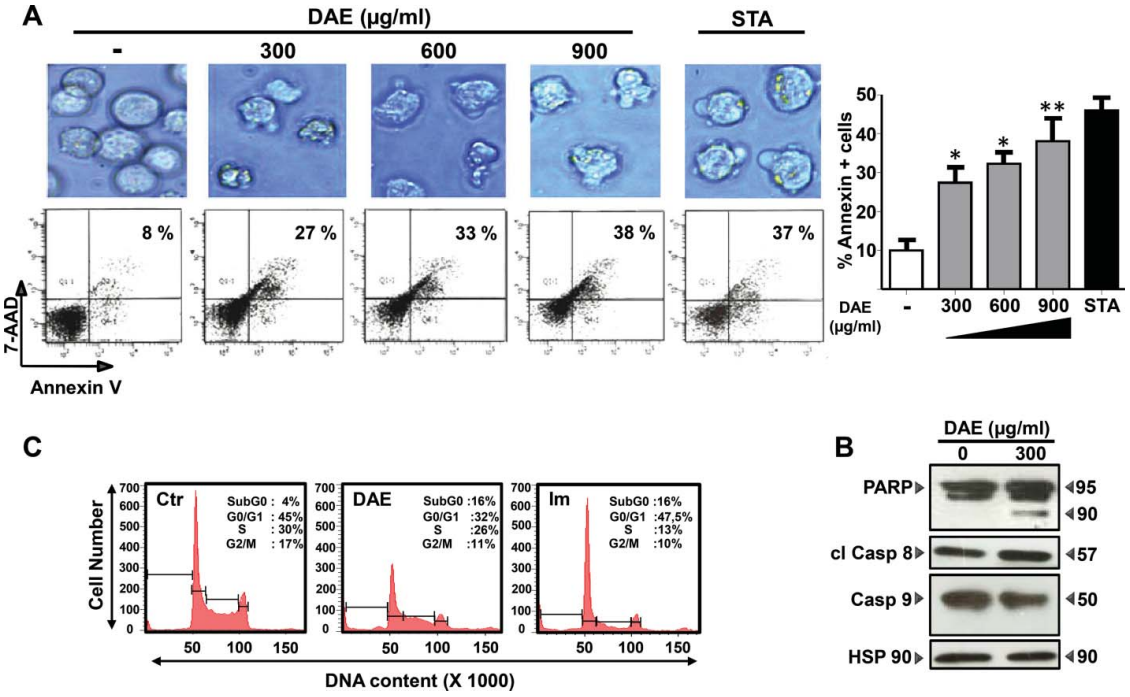

Figure 3. Cell death characterization and cell cycle analysis A: K562 cells were treated with the indicated dose of DAE. Changes in cellular morphology were examined by a light microscope using the phase contrast setting. Apoptotic cells were detected by FACS after Annexin V/7-AAD staining. The cells in the highest right quadrant, which are only positive for Annexin V, represent late apoptotic cells. Histograms summarize the apoptotic effect on K562 cells of the different doses of DAE (300, 600, and 900 μg/ml) after 24-h treatment. 10 μM Staurosporine (STA)-treated cells represent the positive control of apoptosis, B: DAE induces both extrinsic and intrinsic caspase-dependent pathways of apoptosis. DAE decreased the level of the apoptosis-related proteins pro-caspase 9 and increased the ones of the cleaved caspase 8 (cl casp 8) and PARP in K562 cells. HSP90 served as an internal control to monitor protein loading, C: Cell cycle analysis showing subG0, G0/G1, S, and G2M content in untreated K562 cells, cells treated with DAE at 300 μg/ml or with 1 μM Imatinib for 24 h, respectively. Data are reported as the mean $\pm$ SE of three independent experiments ($^{*}P < 0.05$, $^{**}P < 0.01$).

typical morphological changes of apoptosis, cell shrinkage, and membrane blebbing (Fig. 3A). To better verify if DAE treatment induced apoptosis of K562 cells, we have assessed such cell death by flow cytometry after AnnexinV/7-AAD staining. As shown in Fig. 3A, we found that DAE-mediated inhibition of K562 cells growth pass through, at least in part, the induction of apoptosis. Indeed, the percentage of apoptotic cells in response to 300, 600, and 900 μg/ml DAE increased in a dose-dependent manner reaching 27.4%, 32.3%, and 38% ($P < 0.05$) of Annexin-positive cells respectively, compared to the nontreated cells (Fig. 3A). DAE-induced apoptosis of K562 was later supported by cell cycle analysis. We found that exposure to DAE at 300 μg/ml or Imatinib at 1 μM for 24 h resulted in a significant increase in the percentage of K562 cells in the SubG0 phase compared to nontreated cells (Fig. 3C). Taken together, these data showed a direct correlation between the extent of apoptosis and the level of growth inhibition of K562 caused by DAE. To further characterize the molecular mechanism by which DAE induced apoptosis of K562 cells, we monitored, by Western blotting, the changes in apoptotic effectors related to intrinsic and extrinsic pathways in mock and DAE-treated K562 cells. The results showed that DAE induced full caspases cascade activation, as shown by the cleavage of caspase-3 substrate, PARP (Fig. 3B). Moreover, we found that the level of the cleaved form of Caspase-8 increased in DAE-treated K562 cells compared to mock-treated ones, indicating the activation of the canonical extrinsic pathway of apoptosis. DAE treatment has also activated Caspase-9 as shown by the decrease of the level of procaspase 9 (Fig. 3B). Overall, caspases analysis suggests that the DAE-induced apoptosis of K562 cells relies on the induction of both extrinsic and intrinsic pathways of apoptosis.

DAE and Imatinib disturb cell cycle progression in different manners

To better explore the mechanisms through which DAE elicits its growth inhibitory effect, we examined its effect on cell cycle progression of K562 cells over 24 h. Besides the above-indicated increase in sub G0/G1 population, cell cycle analysis showed a DAE-induced decrease in the percentage of the three phases of the cell cycle, G0/

G1, S, and G2/M (Fig. 3C). The percentages of the untreated cells accumulated in these phases were 46%, 30%, and 17%, respectively, while the ones registered in DAE-treated cells were 32%, 26%, and 11%. Such effect was different than the one exerted in Imatinib-treated cells where we found about 65% decrease in S phase (13%), a milder decrease in G2/M phase (10%), and an arrest in G0/G1 phase (47%). These data along with the different level of cell death induction shown in Fig. 3A (upper panel) suggest that DAE and Imatinib affect the cell survival and cell cycle progression in different manners. It is worth to note that the DAE treatment was associated with an increase in the cell cycle inhibitor p27/KIP1, which may explain, at least in part, the disruption of the cell cycle progression of DAE-treated cells (Fig. 4D).

Effect of DAE on the chimeric protein BCR-ABL and its downstream STAT5 and ERK$_{1/2}$

Imatinib is currently the most effective drug against CML. Its effect relies on its direct interaction and inhibition of the tyrosine kinase BCR-ABL, a chimeric protein behind the phenotype of CML and K562 cells (31). In order to check if the DAE inhibitory effect on K562 cells survival passes through the interference with the function of the oncogenic protein BCR-ABL, we analyzed, by Western blotting, its phosphorylation level and the one of its target STAT5 along with the phosphorylation of ERK pathway activation. Interestingly, DAE at 300 μg/ml induced the dephosphorylation of both BCR-ABL and its downstream target STAT5, after 24 h of treatment (Fig. 4A). A rapid blockade of the Raf/MEK/ERK pathway, downstream of BCR-ABL, is commonly found in Imatinib-treated K562 cells (31,32). To investigate the effect of DAE on the ERK$_{1/2}$ pathway, we analyzed the phosphorylation status of ERK$_{1/2}$ over 24-h treatment. Compared to mock-treated cells, DAE (at 300 μg/ml) did not affect the phosphorylation status of ERK$_{1/2}$ within 4 and 8 h of treatment. However, after 24 h, DAE induced a total blockade of ERK$_{1/2}$ phosphorylation (Fig. 4B). K562 cells treated with IM (at 1 μM), for 24 h, were used as a reference drug and positive control for dephosphorylation of ERK$_{1/2}$ and STAT5 kinases

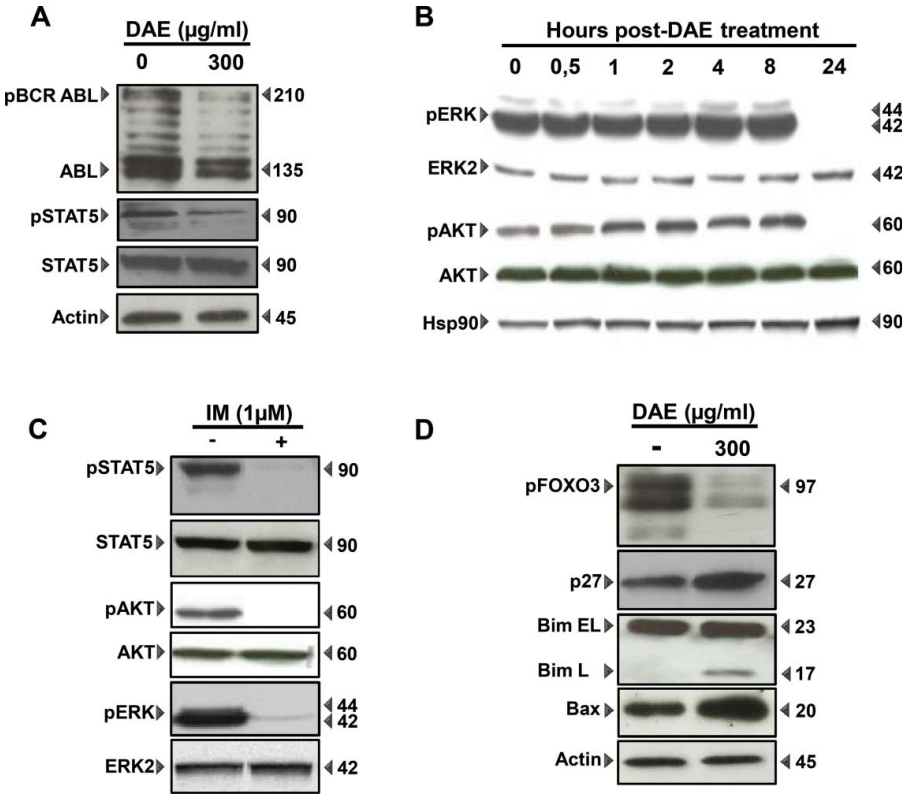

Figure 4. Analysis of cellular effectors targeted by DAE in K562 cells A: Western blotting analysis with the indicated antibodies showed a dephosphorylation of the chimeric oncoprotein BCR-ABL at 300 μg/ml along with the dephosphorylation of its downstream target STAT5, B: A short treatment, of K562 cells, from 0.5 to 8 h with the same dose of DAE did not affect the phosphorylation statue of either AKT or ERK compared to a total blockage of both kinases after 24 h of treatment, C: Treatment of K562 cells with Imatinib (IM), for 24 h, blocked the phosphorylation of STAT5, Akt, and ERK$_{1/2}$, D: DAE-induced dephosphorylation of Akt was associated with the dephosphorylation of its target FOXO3 and the induction of FOXO3 targets, Bim and P27/kip1 along with the increase in Bax expression. One representative experiment of two independent ones was shown.

(Fig. 4C). These results suggest that the DAE-mediated decrease in kinase activity of the chimeric protein BCR-ABL led to the blockade of its target STAT5 and the $ERK_{1/2}$ pathway.

DAE decreases K562 cell proliferation by targeting Akt survival pathway and its target FOXO3 transcription factor

In order to verify whether the DAE-mediated modulation of K562 cell proliferation and survival passes through the interference with the major cell survival pathway, PI3K/Akt, we checked the phosphorylation status of Akt in Mock and DAE-treated cells. Our data showed that, similar to $ERK_{1/2}$ kinetic, DAE did not affect Akt phosphorylation after 4 and 8 h of treatment, while a prolonged treatment for 24 h induced a total dephosphorylation of Akt (Fig. 4B). Cells treated with Imatinib (at 1 μM) for 24 h were used as a positive control for a total blockade of Akt (Fig. 4C). One way by which Akt inhibits cell apoptosis is the phosphorylation/inactivation of FOXO3, while Akt inactivation leads to the accumulation of the dephosphorylated form of FOXO3 in the nucleus where it activates the transcription of multiple proapoptotic genes, like Bim and Bax (33,34) as well as genes controlling cell cycle progression, such as p27 (35). As shown in Fig. 4D, cells exposed to DAE exhibited a pronounced reduction in the phosphorylation state of the Akt target site on FOXO3, threonine 32. Interestingly, we found that such dephosphorylation was also associated with the induction of FOXO3 targets, the proapototic effectors Bim and Bax and the cell cycle inhibitor p27 (Fig. 4D). These data suggest that DAE-mediated inhibition of K562 proliferation and survival relies, at least in part, on the inhibition of the activity of the prosurvival kinase Akt, causing the activation of FOXO3, which induced the expression of the proapoptotic effectors Bim and Bax and the cell cycle inhibitor p27.

DAE decreases the VEGF secretion level of K562 cells

Because CML is considered to be angiogenesis-dependent malignancy and Imatinib was reported to reduce VEGF secretion (36), we asked whether a similar paradigm might exist in DAE-treated K562 leukemia cell. This was supported by the DAE-induced blockade of $ERK_{1/2}$, the kinase controlling VEGF expression (37). We found that treatment of K562 cells with DAE (300 μg/ml) for 24 h induced a slight decrease in VEGF secretion compared to mock-treated cells ($P < 0.05$). Interestingly, the inhibition increased once K562 cells were treated with DAE for 72 h with a 60% reduction

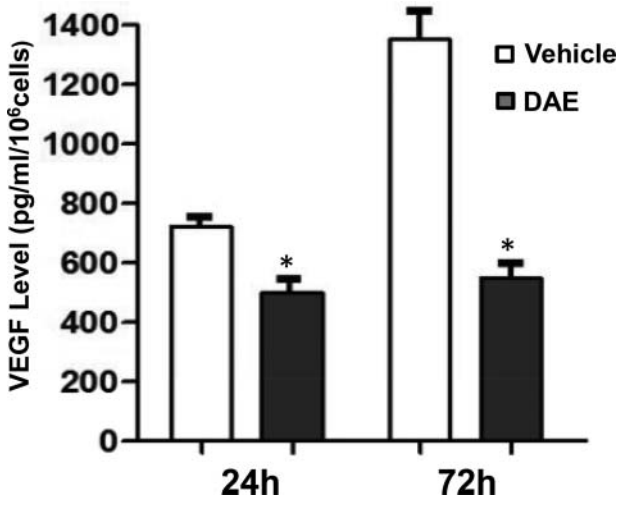

Figure 5. DAE affects VEGF secretion in K562 cells. K562 cells were treated by DAE 300 μg/ml for 1–3 days as indicated. The conditioned medium was collected and VEGF level was determined by a human VEGF ELISA Kit. The result demonstrated a suppression of VEGF secretion in a time-dependent manner upon DAE treatment. Results are reported as the mean ± SE of three independent experiments each run in triplicate ($^*P < 0.05$). The data were corrected to the cell number.

($P < 0.05$) in VEGF secretion (Fig. 5). Thus, DAE exerted a downregulation of VEGF production in a time-dependent manner which may decrease angiogenesis, enhancing the antileukemia effect of DAE.

Discussion

Plant foods are the main sources of bioactive phytochemicals, and their incorporation in the human diet appears to be strongly and inversely related to the onset of several diseases. The use of food-based strategies to achieve optimal dietary requirements promotes the integration of wild vegetables into diets. *A. roseum* is a wild edible plant traditionally gathered and consumed in the Mediterranean regions. Despite numerous studies highlighting the medicinal properties of other plants belonging to the same genus, little is known about the beneficial effectiveness of *A. roseum* (38). Herein, we investigated for the first time the antitumoral effect of *A. roseum* in human CML K562 cells. We found that dried aqueous extract of *A. roseum* extract exerted a potent suppressive effect on K562 cells growth through the dephosphorylation of the oncoprotein BCR-ABL, the inhibition of PI3K/Akt and $ERK_{1/2}$ pathways, and the abrogation of VEGF secretion.

We first demonstrated that DAE exerted the most effective antiproliferative activity in a dose- and time-dependent manner without any toxicity on K562 cells compared to the fresh and DMEs. Moreover, DAE

extract exhibited no toxicity to the normal mouse fibroblasts (NIH3T3) cells. This result is in agreement with Karmakar studies (39), who reported that, compared to tumor cells, normal cells were more resistant to cell death induced by *Allium*-derived organosulfur compounds (OSCs). The plausible explanation for the fact that different extracts from the same plant can be endowed with different antiproliferative activity toward one type of cancer cells is that they have different chemical compositions.

Among the many bioactive compounds identified, organosulfur compounds (RCSO), which are abundant in *Allium* are responsible for the protective effect against different types of cancer (25). We have then explored the level of such compounds in the different fractions used in our study. We found that RCSO decreased during the storage. The profile of aroma components in DAE corresponded to the related pattern of aroma precursors (cysteine sulfoxides) and depended strongly on storage temperatures. Thus, 4°C is considered as the best temperature for the conservation of RCSO as long as organosulfur precursors are still present even after 90 days of storage.

One of the metabolites of garlic, allicin, which is not present in intact plant, is formed upon crushing of garlic bulbs due to an enzymatic reaction between nonprotein amino acid "alliin, a precursor molecule" and the alliinase. This natural occurring enzyme present in the vascular bundle cells of the garlic bulb is released when the bulb tissue is crushed and reacts with the above precursors to release volatile allyl thiosulfinates (40).

Since its discovery (41), thiosulfinate allicin has been the best characterized biologically active compound of garlic and shown to possess a variety of biological activities, including antitumor (42) and immunomodulatory effects (43). We found that at different storage temperatures, DAE presented the highest amount of allicin compared to FAE even after 90 days of storage at different temperatures. This result suggests that the differential inhibitory effect between FAE and DAE toward K562 cell proliferation may due to the presence of more stable sulfur-containing compounds RCSO and allicin in DAE extract.

According to Lagunas and Castaigne, alliin and alliinase must remain separate before eating to preserve the allicin potential inside the body (44). Based on our results, these conditions can be fulfilled only in the dried product (DAE extract) and drying remains the most appropriate technique for the preservation of the organosulfur precursors to avoid this reaction. The decrease of allicin and related thiosulfinates concentration after 7 days of storage at room temperature and 35°C could be explained by the fact that these compounds are highly unstable and instantly decomposed to yield various sulfur compounds including diallyl sulfide, diallyl disulfide (DADS), diallyltrisulfide (DATS), dithiins, and ajoene (45,46).

It is well documented that thiosulfinates (Ti) precursors are markers for the quality determination of *Allium* products (47) and their transformation reaction is favored by crushing and by the presence of water (44). The fact that crushed extract (FAE) exerted only a moderate inhibitory effect on K562 growth over 24 h which disappeared after 72 h (data not shown) of treatment, suggests that all the precursors are transformed into volatile Ti. Thus, we propose that there is a close direct relationship between the antiproliferative activity of DAE and the sulfur-containing compounds RCSO which, contains the highest amount of allicin.

In CML, activation of phosphoinositide 3-kinase (PI3K/Akt), $ERK_{1/2}$, and STAT5 has emerged as essential signaling mechanisms in BCR-ABL-induced leukemogenesis (48). Thus, targeting signaling pathways activated by BCR-ABL is a promising approach for drug development (49).

In K562 cells, the TKI, IM, abolishes BCR-ABL activity and as consequence $ERK_{1/2}$, Akt, and STAT5 activation (31), leading to mitochondria-mediated cell death. We found that, 24 h post treatment, DAE also induced the dephosphorylation of the chimeric protein BCR-ABL and its target STAT5, (Fig. 4A), indicating the modulation of such LMC causing oncoprotein functions. Jacquel *et al.* have previously reported (31) that ERK and STAT5 inhibition in K562 cells treated with 1 μM Imatinib started after 0.5 h post treatment. The authors also highlighted the fact that such effect was maintained after 24 h to reach a total blockade of the studied pathways. However, we found that DAE-mediated blockade of the indicated pathways only occurred 24 h post treatment (Fig. 4B). The absence of DAE effect, on signaling pathways, at shorter time points, may be explained by the fact that it is made of a mixture of bioactive compounds whose concentrations may be much lower than the one of Imatinib (1 μM corresponds to 0.6 μg/ml). We suggest that these compounds mime Imatinib effect on the studied signaling pathways 24 h post DAE treatment. However, we still cannot exclude that DAE effect may also due to the interference with signaling pathways other than those targeted by Imatinib.

In leukemia cells, $ERK_{1/2}$ and PI3K/Akt pathways play a crucial role in regulating cell proliferation, differentiation, survival, and drug resistance through regulation of multiple downstream cascades (4,48). Interestingly, DAE induced a total blockade of Akt and $ERK_{1/2}$ phosphorylation after 24 h of treatment (Fig. 4B).

One way by which Akt enhances cell survival is the phosphorylation/inhibition of FOXO3 transcription factor which when activated would induce apoptosis (34). We have then assessed Akt-mediated FOXO3 phosphorylation in DAE-treated cells and found that such treatment was associated with the dephosphorylation/activation of FOXO3. These data suggest that DAE-induced cell death pass through FOXO3 activation (Fig. 4D). Indeed, Essafi et al. (50) have previously reported that Imatinib-induced cell death of CML pass through FOXO3 activation (50). These investigators have also shown that Imatinib-induced apoptosis of CML relies on FOXO3-mediated induction of the proapoptotic effectors Bim. This also correlates with our data since we found that the short proapoptotic form of Bim was induced in DAE-treated cells. Hence, once activated, FOXO3 promotes the expression of proapoptotic proteins such as Bim to enhance apoptosis cascades. Thus, our data suggest that DAE-induced inhibition of K562 cell growth along with the induction of apoptosis pass through the modulation of BCR-ABL and Akt inhibition, leading to FOXO3-mediated induction of Bim causing cell apoptosis (Fig. 4D). According to the results reported by Yang et al. (51), ERK prosurvival effect also relies on FOXO3 phosphorylation. Indeed, ERK-mediated phosphorylation of FOXO3 targets its MDM2-mediated proteolysis. Therefore, our data suggest that the DAE-induced dephosphorylation of $ERK_{1/2}$ may enhance the stability of FOXO3, contributing to its proapotoptic effect.

The proapoptotic BH3-only protein Bim activates the proapoptotic protein Bax and induces a mitochondrial dysfunction (52). During apoptosis, Bax moves from cytosol to mitochondria and causes release of proapoptotic factors with subsequent caspases activation and DNA fragmentation (53). Interestingly, we found that in K562 cells, DAE was able to induce Bim activation, upregulate Bax expression, and induce PARP cleavage and caspases 3 and 9 activation, indicating a mitochondrial cell death (Fig. 3B). Simultaneously, we found that caspase 8 was also activated in DAE-treated cells, revealing the involvement of the extrinsic pathway in DAE-induced apoptosis (Fig. 3B). Our data correlate with the ones of Park and collaborators (54) who reported that hexane extract of aged black garlic HABGE (aged black garlic extract ABGE, which is produced by a long-term extraction from garlic with hexane) induced the activation of caspase 9 and caspase 8, accompanied by proteolytic degradation of PARP in human leukemic cells U937 (55). Additionally, we found that DAE inhibited the proliferation of K562 cells through cell cycle disturbance, which was associated with an increase of p27/Kip1 expression (Fig. 4D). Our results are in accordance with Drullion's work who reported that treatment of K562 cells with IM (1 μM) during 48 h induced cell cycle arrest and p27/Kip1 expression increase (5). These data better support our finding regarding the involvement of FOXO3 in DAE inhibitory effect on K562 cell proliferation and survival because p27/Kip1 is also a target of FOXO3.

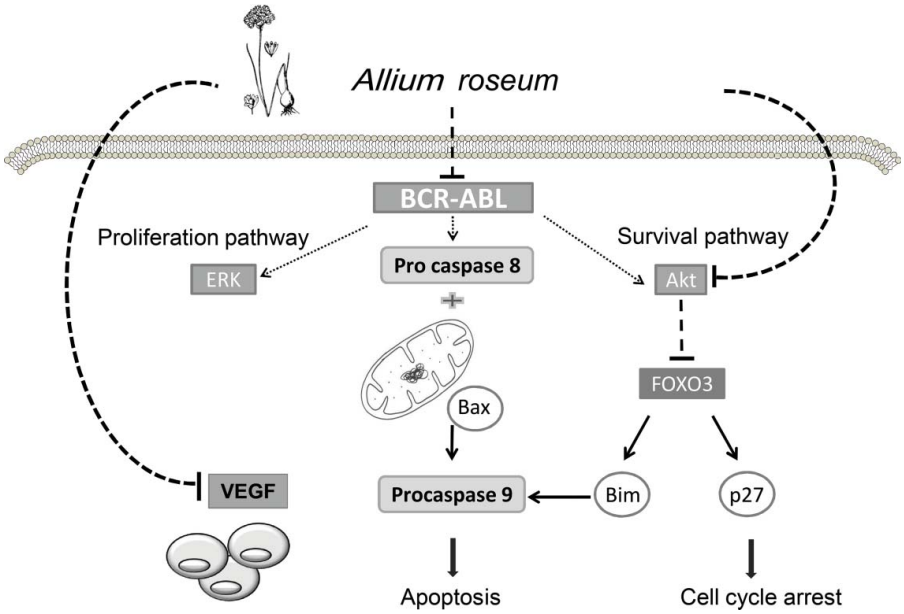

Figure 6. Schematic model for the mechanisms of DAE exerted antitumor activity on K562 cells. The DAE extract controls K562 cell viability by modulating the activity of different targets. Continuous arrows indicate activation while discontinuous arrows indicate inhibition exerted by DAE.

Analysis of the chemical composition of the different extracts used in our study revealed a high amount of allicin in DAE, compared to FAE, suggesting allicin to be responsible for cell death induced by DAE. Consistent with our finding, previous study indicated that allicin induced mitochondrial release of cytochrome C, activation of caspases 9 and 3, and DNA fragmentation in Human leukemia cells lines HL60 and U937 in a concentration- and time-dependent manner (55). However, we still cannot exclude that other components may be behind the DAE effect and that further extensive analysis of DAE composition should be performed in order to identify the molecules involved in DAE effects.

It is well documented that the growth of malignant tissues depends on angiogenesis. Various studies showed that angiogenesis played a pivotal role in leukemia (56). VEGF, which functions in both an autocrine and paracrine manner, is one of the most potent inducers of angiogenesis during leukemia cell growth and angiogenesis. Interestingly, we found that DAE targeted such an important growth factor involved in proliferation and invasion of tumor cells by decreasing its secretion in a time-dependent manner (Fig. 5). In accordance with the fact that PI3K/Akt pathway can be regulated in an autocrine manner by various growth factors, such as VEGF (3), our data suggest that the modulation of PI3K/Akt pathway by DAE might be mediated by the inhibition of VEGF rather than a direct effect. Most importantly, IM has been also reported to downregulate the expression of VEGF in K562 cells in a dose-dependent manner (36).

In conclusion, our study provides support for the potential utility of dehydrated *A. roseum* against leukemia. We described for the first time the ability of *A. roseum* dried aqueous extract to inhibit the proliferation of K562 CML cell line. This activity required a negative modulation of the chimeric oncoprotein BCR-ABL, which led to the inhibition of both $ERK_{1/2}$ and PI3K/Akt signaling pathways and the induction of caspase-dependent apoptosis through its extrinsic and intrinsic pathways (Fig. 6). Furthermore, *A. roseum* might be endowed with an antiangiogenic activity as it was able to induce downregulation of VEGF production by K562 cells (Fig. 6). It is worth to note that, the fact that we found DAE to be less toxic than the currently used drug Imatinib, suggests that such extract may be even more efficient and safer than Imatinib. Recommendations for daily alliin or allicin uptake vary widely between 4 and 12 mg of alliin and 2 and 5 mg of allicin (55).

In Japan and West countries, garlic products have been popular and marketed in recent years as healthy foods with beneficial physiological effects for humans. Consequently, the majority of the garlic supplements sold today is garlic powder tablets that are standardized on allicin (57).The above data suggest that the drying methods gave superior quality product of rosy garlic and then can be considered as the optimal treatment process that we can propose to preserve *A. roseum*. Overall, our study proposes DAE as an additive, cost-effective non-toxic product that may help treating and/or preventing CML.

Declaration of interest

The authors declare that they have no competing interests.

Funding

This work was supported by the Tunisian Ministry of Higher Education and Scientific Research (LR11IPT04). The funders had no role in study design, data analysis, decision to publish, or preparation of the manuscript.

References

1. Middleton MK, Zukas AM, Rubinstein T, Michele J, Peijuan Z, et al.: Identification of 12/15-lipoxygenase as a suppressor of myeloproliferative disease. *J Exp Med* **203**, 2529–2540, 2006.
2. Deininger MW, Vieira S, and Mendiola R: BCR ABL tyrosine kinase activity regulates the expression of multiple genes implicated in the pathogenesis of chronic myeloid leukemia. *Cancer Res* **60**, 2049–2055, 2000.
3. Okumura N, Yoshida H, Kitagishi Y, Murakami M, and Nishimura Y: PI3K/AKT/PTEN signaling as a molecular target in leukemia angiogenesis. *Adv Hematol* **2012**(5), 84308, 2012.
4. Johnson GL, and Lapadat R: Mitogen-activated protein kinase pathways mediated by ERK, JNK, and p38 protein kinases. *Science* **298**, 1911–1912, 2002.
5. Drullion C, Trégoat C, Lagarde V, Tan S, Gioia R, et al.: Apoptosis and autophagy have opposite roles on imatinib-induced K562 leukemia cell senescence. *Cell Death Dis* **3**, e373, 2012.
6. O'Hare T, Eide CA, and Deininger MW: Bcr-Abl kinase domain mutations, drug resistance, and the road to a cure for chronic myeloid leukemia. *Blood* **110**, 2242–2249, 2007.
7. Rivlin RS: Historical perspective on the use of garlic. *J Nutr* **131**, 951–954, 2001.
8. Thomson M, and Ali M: Garlic [*Allium sativum*]: a review of its potential use as an anti-cancer agent. *Curr Cancer Drug Target* **3**, 67–81, 2003.
9. Cuenod A: Flore de la Tunisie. *Eds Office de l'Experimentation et de la Vulgarisation Agricole de Tunisie* **287**, 1954.
10. Le Floc'h E: Contribution à une étude ethnobotanique de la flore tunisienne. *Programme flore et végétation tunisienne*. Tunis: Ministère de l'Enseignement Supérieur et de la Recherche Scientifique, 1983.
11. Najjaa H, Neffati M, Zouari S, and Emmar E: Essential oil composition and antibacterial activity of different extract

of *Allium roseum* L a North African endemic species. *CR Chim.* **10**, 820–826, 2007.
12. Najjaa H, Fattouch S, Ammar E, and Neffati M: Antimicrobial potentials of Allium species: Recent Advances and Trends. "Science against microbial pathogens: communicating current research and technological advances", Antonio Méndez-(Ed.), *Formatex Research Center* **2**, 1205–1210, 2011.
13. Najjaa H, Fattouch S, Ammar E, and Neffati M: Allium species, ancient health food for future. *Sci Health Soc Aspects Food Chem* **17**, 343–354, 2012.
14. Najjaa H, Zerria K, Fattouch S, Ammar E, and Neffati M: Antioxidant and antimicrobial activities of *Allium roseum* L. "Lazoul", a wild edible endemic species in North Africa. *Int J Food Prop* **14**, 371–380, 2011.
15. Arnault I, Huchette O, and Auger J: Characterisation of aroma "type" in Allium species according to their S-alk (en)yl cysteine sulfoxides and γ-glutamyl dipeptides contents. *Acta Hortic* **853**, 171–182, 2010.
16. Keusgen M, Schulz H, Glodek J, Krest I, Krüger H, et al.: Characterization of some *Allium* hybrids byaroma precursors, aroma profiles, and alliinase activity. *J Agric Food Chem* **50**, 2884–2890, 2002.
17. Kamenetsky R, London Shafir I, Khassanov F, Kik C, van Heusden AW, et al.: Diversity in fertility potential and organo-sulphur compounds among garlics from Central Asia. *Biodivers Conserv* **14**, 281–295, 2005.
18. Arnault I, Christidès JP, Mandon N, Haffner T, Kahane R, et al.: High-performance ion-pair chromatography method for simultaneous analysis of alliin, deoxyalliin, allicin and dipeptide precursors in garlic products using multiple mass spectrometry and UV detection. *J Chromatogr A* **991**, 69–75, 2003.
19. Sundaram SG, and Milner JA: Impact of organosulfur compound in garlic on canine mammary tumor cells in culture. *Cancer Lett* **74**, 85–90, 1993.
20. Sundaram SG, and Milner JA: Diallyl disulfide induces apoptosis of human colon tumor cells. *Carcinogenesis* **17**, 669–673, 1996.
21. Rabinkov A, Miron T, Konstantinovski L, Wilchek M, Mirelman D, et al.: The mode of action of allicin: trapping of radicals and interaction with thiol containing proteins. *Biochim Biophys Acta* **1379**, 233–244, 1998.
22. Oommen S, Anto RJ, Srinivas G, and Karunagaran D: Allicin (from garlic) induces caspase-mediated apoptosis in cancer cells. *Eur J Pharmacol* **485**, 97–103, 2004.
23. Park B, Kim K, Rhee DK, and Pyo S: The apoptotic effect of allicin in MCF-7 human breast cancer cells: role for ATF3. *FASEB J* **26**, lb367, 2012.
24. Miron T, Shin I, Feigenblat G, Weiner L, and Mirlman D: A spectrophotometric assay for allicin, alliin, and alliinase (alliin lyase) with a chromogenic thiol: reaction of 4-mercaptopyridine with thiosulfinates. *Anal Biochem* **307**, 76–83, 2001.
25. De Gianni, and Fimognari C: Anticancer mechanism of sulfur-containing compounds. *Enzymes* **37**, 167–92, 2015.
26. Amagase H: Clarifying the real bioactive constituents of garlic. *J Nutr* **136**, 716–725, 2006.
27. Patya M: Allicin stimulates lymphocytes and elicits an antitumor effect: A possible role of p21ras. *Int Immunol* **16**, 275–281, 2004.
28. Borlinghaus J, Albrecht F, Gruhlke MCH, Nwachukwu ID, Slusarenko AJ: Allicin: Chemistry and biological properties. *Molecules* **19**, 12591–12618, 2014.
29. Arnault I, and Auger J: Seleno compounds in garlic and onion. *J Chromatogr A* **1–2**, 23–30, 2006.
30. Bruggisser R, von Daeniken K, Jundt G, Schaffner W, and Tuliberg-Reinert H: Interference of plant extracts, phytoestrogens and antioxidants with the MTT tetrazolium assay. *Planta Med* **68**, 445–448, 2002.
31. Jacquel A, Herrant M, Legros L, Belhacene N, Luciano F, et al.: Imatinib induces mitochondria dependent apoptosis of the Bcr-Abl-positive K562 cell line and its differentiation toward the erythroid lineage. *FASEB J* **17**, 2160–2162, 2003.
32. Ma L, Shan Y, Bai R, Xue L, Christopher A, et al.: Green. A therapeutically targetable mechanism of BCR-ABL independent imatinib resistance in chronic myeloid leukemia. *Sci Transl Med* **6**, 252ra121, 2014.
33. Gilley J, Coffer PJ, and Ham J: FOXO transcription factors directly activate bim gene expression and promote apoptosis in sympathetic neurons. *J Cell Biol* **162**, 613–622, 2003.
34. Brunet A, Bonni A, Zigmond MJ, Lin MZ, Juo P, et al.: Akt promotes cell survival by phosphorylating and inhibiting a forkhead transcription factor. *Cell* **96**, 857–868, 1999.
35. Stahl M, Dijkers PF, Kops GJ, Lens SM, Coffer PJ, et al.: The forkhead transcription factor FoxO regulates transcription of p27Kip1 and Bim in response to IL-2. *J Immunol* **168**, 5024–5031, 2002.
36. Legros L, Bourcier C, Jacquel A, Mahon F X, Cassuto JP, et al.: Imatinib mesylate (STI571) decreases the vascular endothelial growth factor plasma concentration in patients with chronic myeloid leukemia. *Blood* **104**, 495–501, 2004.
37. Pages G, Milanini J, Richard DE, Berra E, Gothie E, et al.: Signaling angiogenesis via p42/p44 MAP kinase cascade. *Ann N Y Acad Sci* **902**, 187–200, 2000.
38. Howard EW, Ling MT, Chua CW, Cheung HW, Wang X, et al.: Garlic-derived S-allylmercaptocysteine is a novel in vivo antimetastatic agent for androgen-independent prostate cancer. *Clin Cancer Res* **13**, 1847–1856, 2007.
39. Karmakar S, Banik NL, Patel SJ, and Ray SK: Garlic compounds induced calpain and intrinsic caspase cascade for apoptosis in human malignant nuroblastoma SH-Sy5Y cells. *Apoptosis* **12**, 671–684, 2007.
40. Lawson LD, and Gardner CD: Composition, stability, and bioavailability of garlic products used in a clinical trial. *J Agric Food Chem* **51**, 5774–5779, 2005.
41. Cavallito CJ, and Bailey JH: Allicin, the antibacterial principle of *Allium sativum*. I. Isolation, physical properties and antibacterial action. *J Am Chem Soc* **66**, 1950–1951, 1944.
42. Park BJ, Cho SJ, Kwon HC, Lee KR, Rhee DK, et al.: Caspase-independent cell death by allicin in human epithelial carcinoma cells: involvement of PKA. *Cancer Lett* **224**, 123–132, 2005.
43. Lang A, Lahav M, Sakhnini E, Barshack I, Herma H. Fidder, et al.: Allicin inhibits spontaneous and TNF-α induced secretion of proinflammatory cytokines and chemokines from intestinal epithelial cells. *Clin Nutr* **23**, 1199–1208, 2004.

44. Lagunas LLM, and Castaigne F: Effect of temperature cycling on allinase activity in garlic. *Food Chem* **111**, 56–60, 2008.
45. Block E: The chemistry of garlic and onions. *Sci Am* **252**, 114–119, 1985.
46. Gonzalez RE, Burba JL, and Camargo AB: A physiological indicator to estimate allicin content in garlic during storage. *J Food Biochem* **37**, 449–455, 2013.
47. Ichikawa M, Ide N, and Ono K: Changes in organosulfur compounds in garlic cloves during storage. *J Agric Food Chem* **54**, 4849–4854, 2006.
48. McCubrey JA, Steelman LS, Franklin RA, Abrams SL, Chappell WH, et al.: Targeting the RAF/MEK/ERK, PI3K/AKT and p53 pathways in hematopoietic drug resistance. *Adv Enzyme Regul* **47**, 64–103, 2007.
49. Patel D, Suthar MP, Patel V, and Singh R: BCR ABL kinase inhibitors for cancer therapy. *Int J PharmSci Drug Res* **2**, 80–90, 2010.
50. Essafi A, Fernandez de Mattos S, Hassen YA, Soeiro I, et al.: Direct transcriptional regulation of Bim by FoxO3a mediates STI571-induced apoptosis in BcrAbl-expressing cells. *Oncogene* **24**, 2317–2329, 2005.
51. Yang JY, Zong CS, Xia W, Yamaguchi H, Ding1 Q, et al.: ERK promotes tumorigenesis by inhibiting FOXO3a via MDM2-mediated degradation. *Nat Cell Biol* **10**, 138–148, 2008.
52. Shukla S, Rizvi F, Raisuddin S, and Kakkar P: FoxO proteins' nuclear retention and BH3-only protein Bim induction evoke mitochondrial dysfunction-mediated apoptosis in berberine-treated HepG2 cells. *Free Radic Biol Med* **76**, 185–199, 2014.
53. Tzifi F, Economopoulou C, Gourgiotis D, Ardavanis A, Papageorgiou S, et al.: The role of BCL2 family of apoptosis regulator proteins in acute and chronic leukemia. *Adv Hematol* **2012**, 524308, 2012.
54. Park C, Park S, Chung YH, Kim GY, Choi YW, et al.: Induction of apoptosis by a hexane extract of aged black garlic in the human leukemic U937 cells. *Nutr Res Pract* **8**, 132–137, 2014.
55. Miron T, Wilchek M, Sharp A, Nakagaw Y, Naoi M, et al.: Allicin inhibits cell growth and induces apoptosis through the mitochondrial pathway in HL60 and U937 cells. *J Nutr Biochem* **19**, 524–535, 2008.
56. Han Y, Wang X, Wang B, and Jiang G: The progress of angiogenic factors in the development of leukemias. *Intractable Rare Dis Res* **5**(1), 6–16, 2016.
57. Lawson LD, Wang ZJ, and Papadimitriou D: Allicin release under simulated gastrointestinal conditions from garlic powder tablets employed in clinical trials on sterum cholesterol. *Planta Med* **67**, 13–18, 2001.